

VILNIUS UNIVERSITY
CENTER FOR PHYSICAL SCIENCES AND TECHNOLOGY
INSTITUTE OF CHEMISTRY

Andrius Budreika

The study of the electrodeposition of Ni, Co and their alloys with tungsten and molybdenum

Summary of Doctoral Dissertation

Physical sciences, chemistry (03 P)

Vilnius, 2010

The work was carried out in Vilnius University in the period of 2006 – 2010.

Scientific supervisors:

Doc. dr. Henrikas Cesiulis (Vilnius University, Physical sciences, Chemistry – 03P).

Chairman:

Prof. habil. dr. Aivaras Kareiva (Vilnius University, Physical sciences, Chemistry – 03P);

Members:

Prof. habil.dr. Gintaras Baltrūnas (Vilnius University, Physical sciences, Chemistry – 03P)

Prof. habil. dr. Albertas Malinauskas (Institute of Chemistry Center For Physical Sciences And Technology, Physical sciences, Chemistry – 03P)

Prof. habil. dr. Algimantas Undzėnas (Physics Institute Center For Physical Sciences And Technology, Physical sciences, Physics – 02P)

Dr. Evaldas Naujalis (Semiconductor Physics Institute Center for Physical Sciences and Technology, Physical sciences, Chemistry – 03P)

Official opponents:

Doc. dr. Nijolė Dūkštienė (Kaunas University of Technology, Physical sciences, Chemistry – 03P)

Doc. dr. Darius Jasaitis (Vilnius University, Physical sciences, Chemistry – 03P)

The official discussion will be held on 4 p.m. September 30, 2010 at the meeting of the Evaluation Board at the Auditorium of Inorganic Chemistry of the Faculty of Chemistry of Vilnius University.

Address: Naugarduko 24, LT-03225 Vilnius, Lithuania.

Tel.: 231 15 72. Fax.: 233 09 87.

The summary of doctoral dissertation was mailed on the 27 of August 2010.

The dissertation is available at the Library of Vilnius University and the Library of Institute of Chemistry.

VILNIAUS UNIVERSITETAS
FIZINIŲ IR TECHNOLOGIJOS MOKSLŲ CENTRO
CHEMIJOS INSTITUTAS

ANDRIUS BUDREIKA

Ni, Co bei jų lydinių su volframu ir molibdenu elektronusodavimo tyrimas

Daktaro disertacija
Fiziniai mokslai, chemija (03 P)

Vilnius, 2010

Disertacija rengta 2006 – 2010 metais Vilniaus universitete.

Mokslinis vadovas:

Doc. dr. Henrikas Cesiulis (Vilniaus universitetas, fiziniai mokslai, chemija – 03 P).

Disertacija ginama Vilniau universiteto Chemijos mokslo krypties taryboje:

Pirmininkas

Prof. habil. dr. Aivaras Kareiva (Vilniaus universitetas, fiziniai mokslai, chemija – 03 P);

Nariai:

Prof. habil.dr. Gintaras Baltrūnas (Vilniaus universitetas, fiziniai mokslai, chemija – 03 P)

Prof. habil. dr. Albertas Malinauskas (Fizinių ir technologijos mokslų centro Chemijos institutas, fiziniai mokslai, chemija – 03P)

Prof. habil. dr. Algimantas Undzėnas (Fizinių ir technologijos mokslų centro Fizikos institutas, fiziniai mokslai, fizika – 02P)

Dr. Evaldas Naujalis (Fizinių ir technologijos mokslų centro Puslaidininkų fizikos institutas, fiziniai mokslai, chemija – 03P)

Oponentai:

Doc. dr. Nijolė Dūkštienė (Kauno technologijos universitetas, fiziniai mokslai, chemija – 03P)

Doc. dr. Darius Jasaitis (Vilniaus universitetas, fiziniai mokslai, chemija – 03 P)

Disertacija bus ginama viešame Chemijos mokslo krypties tarybos posėdyje 2010m.

Rugsėjo 30d. 16val. Vilniaus universiteto Chemijos fakulteto Neorganinės chemijos auditorijoje.

Adresas: Naugarduko 24, LT-03225 Vilnius, Lietuva. Tel.: 231 15 72. Faksas: 233 09 87.

Disertacijos santrauka išsiųsta 2010m. Rugsėjo 27d.

Su disertacija galima susipažinti Vilniaus universiteto ir Chemijos instituto bibliotekose.

1. INTRODUCTION

In the meantime the great attention is focused on the W and Mo alloys with iron group metals, because of their attractive mechanical, anticorrosion, electrical, magnetic and tribologic properties and nanocrystalline structure. The magnetic and mechanical properties of Co-Mo alloys make them promising for application in the microelectronics, e.g. in the applications of microelectromechanical systems (MEMS). The electrochemical forming of MEMS have many advantages over other physical processes, such as a room temperature operation, low energy requirements, fast deposition rates, fairly uniform deposition over complicated shapes, low cost, simple scale-up and easily maintained equipment.

The high melting temperature of tungsten and molybdenum makes the preparation and processing of their alloys by the metallurgical methods very difficult. To prepare the tungsten and molybdenum alloys, other advanced processing methods such as powder metallurgy, chemical vapor deposition, and electrodeposition are used. Electrochemical deposition is the most convenient to get alloys with high melting points, such as tungsten or molybdenum alloys. It is commonly accepted that pure tungsten cannot be deposited from the aqueous solutions, but can be codeposited with iron-group metals. This phenomena was called "induced codeposition". The mechanism of it is still unclear, and one of the reasons is a lack data regarding electroreduction of pure iron group metals. Therefore, the attention on the study of Ni(II) and Co(II) electroreduction from various solutions is paid taking into account the utilization of obtained results for the further study of codeposition of W and Mo alloys with iron group metals.

This work is intended to establish more details concerning relationship: electrodeposition parameters vs. CoW alloys composition and structure. The use of pulse currents (PC) is another way to improve surface morphology, to achieve a more uniform current distribution than by DC plating at the same average deposition rate, to increase the content of tungsten or molybdenum, to reduce porosity of electroplated coatings taking into account their applications in microtechnics devices.

Today materials in microelectronics are frequently selected for their electro-magnetic properties and resistance to corrosion. An additional requirement for materials in microtechnology is an extremely high corrosion resistance. This is due to the continuous decrease in component size, down to the micrometer range. Under such conditions, the resistance to device failure due to even a small amount of ionic contaminants may become a key issue in terms of lifetime and reliability. Preliminary tests carried out in the Department of Physical Chemistry of Vilnius University show that corrosion resistance or chemical stability of electrodeposited film is not only dependent on the coating composition, but also on crystal structure, grain size, and methods applied to fabricate the coatings. Differences in corrosion rates between metallurgical and electrodeposited pure metals and alloys can be as large as a factor of 10 times. Therefore, there is a need to initiate an in-depth investigation on corrosion. Tungsten and molybdenum alloys show a relatively low hydrogen overvoltage. Taking into account that corrosion of tungsten and molybdenum alloys with iron group metals undergoes with hydrogen depolarization, and the absolute values of both hydrogen evolution reaction and anodic reaction have to be the same during resting of alloy in corrosive media, and obtained the weak passivity of tungsten and molybdenum alloys in air and

neutral solutions may govern the high corrosion rate of these alloys. Therefore, the aim of the present study is to found a correlation between rates of hydrogen evolution and corrosion properties of Co-W and Ni-Mo alloys.

The main aims of the work were following:

1. To investigate Co(II) and Ni(II) in chloride, sulphate, citrate and pyrophosphate solutions in order to determine the origin of the slow electrochemical reaction and estimate possibilities to determine the charge-transfer particles in the pyrophosphate-ammonia solutions;
2. To investigate the influence of electrodeposition conditions on the composition and structure of Co-W alloys;
3. To compare electrodeposition rate of Co-Mo and Co-Mo-P alloys with pure cobalt electrodeposited from the weakly acidic citrate solutions; estimate electrodeposition in the wafers.
4. To determine a correlation between H₂ evolution exchange current and corrosion current for Co-W and Ni-Mo alloys.

Statement for defense:

1. By means of electrochemical impedance spectroscopy defined that electrochemical reduction of Co(II) and Ni(II) compounds in chloride, sulphate, citrate and pyrophosphate solutions are determined by slow charge transfer and adsorption. EI data are fitted to the equivalent circuits simulating slow charge transfer and adsorption ;
2. Based on the different pH and (NH₄)₂SO₄ influence on the deposition rate obtained in pyrophosphate-ammonia solutions the different charge –transfer particles of Co(II) and Ni(II) are considering, namely CoOH⁺ and Ni(NH₃)_{1÷6}²⁺;
3. The values of grain size of Co-W alloys depend rather on the content of W in the alloy than on the electrodeposition conditions. The value of the grain size is in range from tens nm to 4-6 nm, and that change occurs in the narrow range of W content in the alloy;
4. The deposition rates for cobalt–molybdenum coatings electrodeposited from the citrate solutions are sufficiently lower than that for pure cobalt. The deposition rate increases sufficiently when NaH₂PO₂ is added into solution;
5. For Co-W alloys the clear correlation between exchange current for H₂ evolution and corrosion current is obtained, whereas for Ni-Mo alloys such correlation is rather weak.

2. EXPERIMENTAL

The electrochemical experiments were carried out using AUTOLAB302 system with GPES and FRA software. For the deposition a plating cell with two separated anodic compartments was used. The anodes were two plain graphite rods of area ca. 10 cm². The working electrodes were made of pure Cu, Co, Ni, W and Mo wires (Alfa Aesar, purity no less than 99.9%) with working area 1 cm². For some experiments Cu foil substrate of working area 4 cm² was used. Immediately before electrodeposition the surface was mechanically polished, degreased and then activated in dilute sulfuric acid.

The experiments were carried out at room temperature (20 °C) and at 60 °C. For investigation were used: linear voltammetry, chronopotentiometry and electrochemical impedance spectroscopy methods. The scan rate of 2 mV/s was used in voltammetric experiments. Electrochemical impedance spectroscopy spectra obtained in frequency range from 0,050 to 10000 Hz.

The coating morphology was investigated by scanning electron microscopy (Philips XL 30 FEG). Qualitative elemental analysis of the obtained alloys was carried out by energy-dispersive X-ray spectroscopy (EDS). X-ray diffraction analyses were performed to characterize the electrodeposited coatings. A Dron (type 3.0) instrument with Ni filtered Cu-K_{α1} radiation operated at 30 kV and 30 mA ($\lambda=1.54056 \text{ \AA}$) was used at a continuous scan speed of $0.02^\circ 2\theta \text{ s}^{-1}$. The obtained XRD patterns were filtered from Cu signals.

The deposition rate of Co and Ni was expressed in terms of partial current density at certain conditions. Values of partial current density (j_{Me}) for the Co or Ni and electrodeposition conditions was calculated based on the Faraday law of electrolysis using a following equation:

$$j_{Mg} = \frac{2mF}{MtA} \quad (1)$$

where m is a weight of deposit; F is a Faraday constant; M is a molecular weight of the depositing metal (Co or Ni); t is a deposition time; A is a working area of cathode.

Table 1. Equilibrium constants used for calculations (β is cumulative complex stability constant, K is ionization constant).

Particle	log β or logK	Particle	log β or logK	Particle	log β or logK
NiP ₂ O ₇ ²⁻	5,94	CoP ₂ O ₇ ²⁻	6,1	NiH ₂ Citrat ⁺	1,75
NiHP ₂ O ₇ ⁻	3,71	CoHP ₂ O ₇ ⁻	3,4	NiHCitrat	3,3
Ni(P ₂ O ₇) ₂ ⁶⁻	2,0			NiCitrat ⁻	5,4
NiOH ⁺	3,58	CoOH ⁺	4,2	Ni ²⁺ :SO ₄ ²⁻	2,32
Ni(OH) ₂	8,1	Co(OH) ₂	8,5	CoH ₂ Citr ⁺	1,25
Ni(OH) ₃ ⁻	11,2	Co(OH) ₃ ⁻	9,66	CoHCitrat	3,02
Ni(OH) ₄ ²⁻	11,9	Co(OH) ₄ ²⁻	9,54	CoCitrat ⁻	5,0
NiNH ₃ ²⁺	2,81	CoNH ₃ ²⁺	2,1	Co ²⁺ :SO ₄ ²⁻	2,47
Ni(NH ₃) ₂ ²⁺	5,08	Co(NH ₃) ₂ ²⁺	3,67	NH ₄ ⁺	9,4
Ni(NH ₃) ₃ ²⁺	6,85	Co(NH ₃) ₃ ²⁺	4,78	H ₄ P ₂ O ₇	0,8
Ni(NH ₃) ₄ ²⁺	8,12	Co(NH ₃) ₄ ²⁺	5,53	H ₂ P ₂ O ₇ ²⁻	5,4
Ni(NH ₃) ₅ ²⁺	8,93	Co(NH ₃) ₅ ²⁺	5,75	H ₃ P ₂ O ₇ ⁻	1,4
Ni(NH ₃) ₆ ²⁺	9,08	Co(NH ₃) ₆ ²⁺	5,14	HP ₂ O ₇ ³⁻	7,43

The ionic composition of solution was studied by means of mathematical simulation using “Maple 6” software. For this purpose an appropriate mathematical model has been developed. This model includes a system of equations containing three types of relations, namely: equilibrium constants for all compounds added, including the ionization constants for acids and ammonia, cumulative complex stability constants; mass balance

for all forms in the equilibrium mixture and charge balance. The critically selected equilibrium constants used in this study are listed in Table 1.

3. RESULTS AND DISCUSSION

3.1. The Study of Ni(II) and Co(II) Electroreduction

3.1.1. The ionic composition of solution

For the electrodeposition study of Ni(II) and Co(II) there was selected 4 types of metal M (Co or Ni) solutions:

- 1) chloride: 0,25 mol/l MCl_2 + 0,4 mol/l NaCl + 0,25 mol/l H_3BO_3 pH 6;
- 2) sulphate: 0,25 mol/l MSO_4 + 0,5 mol/l Na_2SO_4 + 0,645 mol/l H_3BO_3 pH 6;
- 3) citrate: 0,25 mol/l MCl_2 + 0,4 mol/l H_3BO_3 + 0,4 mol/l $Na_3C_6H_5O_7$ pH 6;
- 4) pyrophosphate: 0,36 mol/l $Na_4P_2O_7$ + 0,37 mol/l NH_4Cl + 0,14 mol/l MSO_4 pH 8

The ionic compositions were calculated for all solutions. Fig 1 and 2 there are example of ionic composition dependency from pH.

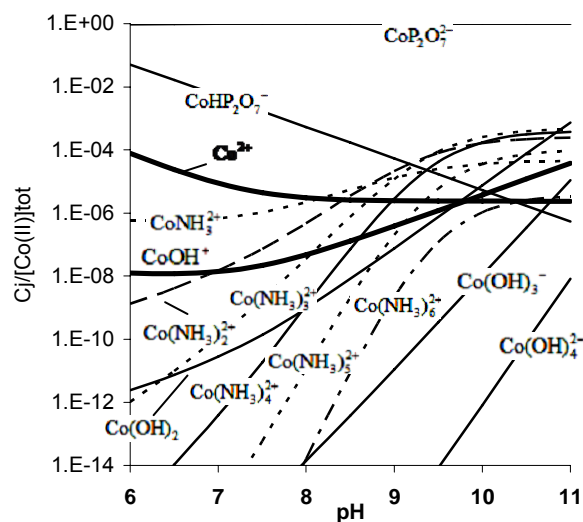
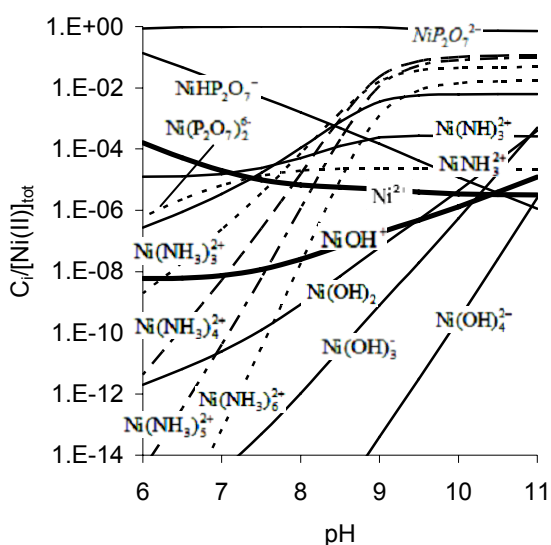


Fig. 1. Calculated partial molar fractions of Ni(II) particles in pyrophosphate solution.

Fig. 2. Calculated partial molar fractions of Co(II) particles in pyrophosphate solution.

Table 2. Calculated M^{2+} and MOH^+ ions concentrations at pH 6.

Solution	Co^{2+} , mol/l	$CoOH^+$, mol/l	Ni^{2+} , mol/l	$NiOH^+$, mol/l
Chloride	0,25	$4,0 \cdot 10^{-5}$	0,25	$9,5 \cdot 10^{-6}$
Sulphate	$1,1 \cdot 10^{-3}$	$1,8 \cdot 10^{-7}$	$1,5 \cdot 10^{-3}$	$6,0 \cdot 10^{-8}$
Citrate	$1,9 \cdot 10^{-5}$	$3,0 \cdot 10^{-9}$	$7,6 \cdot 10^{-6}$	$2,9 \cdot 10^{-10}$
Pyrophosphate	$1,9 \cdot 10^{-6}$	$3,1 \cdot 10^{-10}$	$2,3 \cdot 10^{-5}$	$8,6 \cdot 10^{-10}$

3.1.2 Investigations of voltammetry and electrochemical impedance spectroscopy (EIS)

At the same total metal M(II) concentration the polarization are different: the polarization of electrode at the same current density is bigger when concentrations of M^{2+} and MOH^+ are less (Fig 3 and 4).

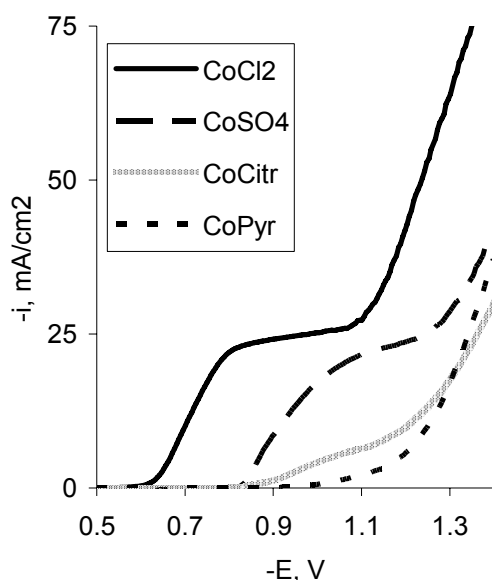


Fig. 3. Polarization curves of Co electrode in chloride (CoCl₂), sulphate (CoSO₄), citrate (CoCitr) and pyrophosphate (CoPyr) solutions.

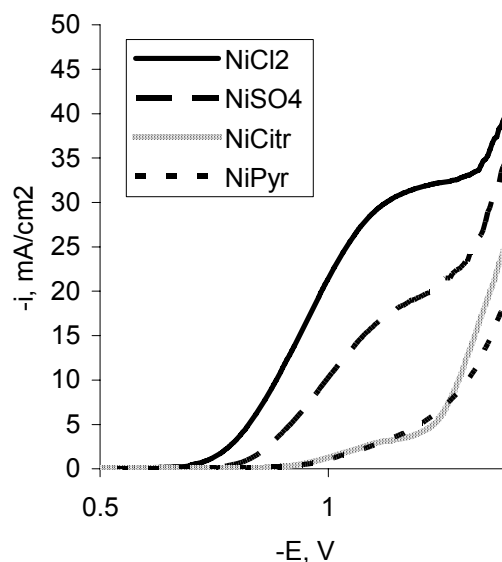


Fig. 4. Polarization curves of Ni electrode in chloride (NiCl₂), sulphate (NiSO₄), citrate (NiCitr) and pyrophosphate (NiPyr) solutions.

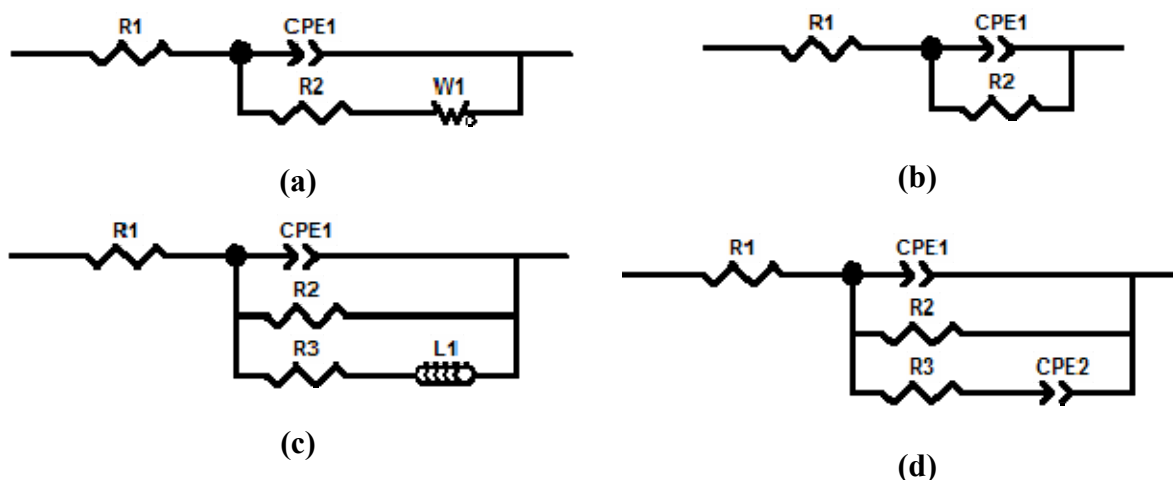


Fig. 5. Equivalent circuits used for fitting results of obtained EI spectra. The physical meaning of the elements of equivalent electric circuits are following: R₁ is a resistance of solution; R₂ is a resistance of charge transfer; CPE1 is an electrical double layer capacity; W₁ is a diffusion impedance modeling element; CPE2 is an adsorption capacity, R₃ – resistance of adsorption (circuit 20d), or resistance that together with R₂ modeling resistance of charge transport (circuit 20c). In this case the resistance of charge transfer (R_p) is calculated by: $R_p^{-1} = R_2^{-1} + R_3^{-1}$.

The shapes of polarization curves are similar to polarization curves with mixed kinetics. However, EI spectra obtained for Co(II) and Ni(II) solutions are different from the spectra with mixed kinetics (except a some spectra for Ni chloride and sulphate solutions), and they fit well to the equivalent circuits simulating a slow charge transport with adsorption (Fig. 5). The example of EI spectra in Nyquist and Bode coordinates and fitting results to the corresponding equivalent circuits is shown in Fig 6. The values for the elements of equivalent circuits for Co(II) and Ni (II) solutions were determined and discussed.

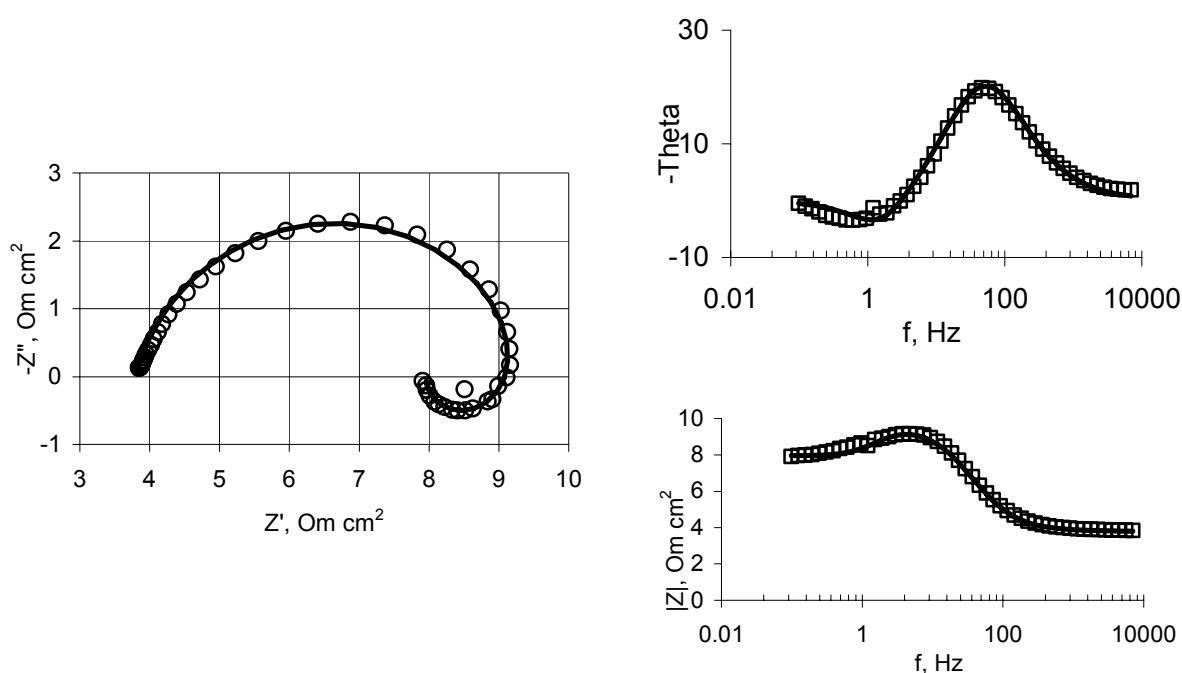


Fig. 6. Experimental EI spectra in Nyquist (left) and Bode (right) coordinates, obtained for Co in chloride solution at $E=-0,70$ V and fitting to the equivalent circuits. Dots – experimental data, line – modeled data according equivalent electric circuit., equivalent electric circuit fig 20 c.

3.1.2 Determination of electrochemically active complex in Ni(II) and Co(II) pyrophosphate solutions

For more detailed investigation was selected pyrophosphate solution because of their actuality for Co-Mo alloys electrodeposition. The study was carried out in solutions, containing 0.36 mol/l $\text{Na}_4\text{P}_2\text{O}_7$ and 0.14 mol/l NiSO_4 or 0.025 mol/l CoSO_4 . The values of total current density were chosen close to that applied for electrodeposition of Mo or W alloys with iron group metals. The values of solution pH ranged from 6 to 9. Ammonium sulfate was used as a source of ammonia as a ligand which is forming in the solution. Initial concentrations $[(\text{NH}_4)_2\text{SO}_4]_0$ were ranged 0 to 0.45 mol/l.

The different influence of pH on the deposition rate of Ni and Co from the solutions without $(\text{NH}_4)_2\text{SO}_4$ was found (Fig. 7). The rate of Co deposition is increasing in pH range from 5 to 8, and then decreases at $\text{pH} > 8$. The decreasing in rate of Co deposition at $\text{pH} > 8$ probably is caused by the peculiarities of hydrogen evolution on the electrode from the alkaline solutions. In contrary, the values of pH do not have influence on Ni deposition rate which values are extremely low. Noticeably, Co deposition rate is few

times higher than that for Ni regardless the sufficiently lower concentration of Co (II) in the solution.

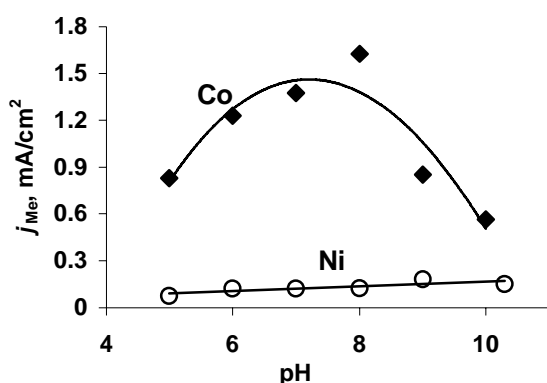


Fig. 7. Partial current densities for Ni and Co electrodeposition as a function of pH obtained from the pyrophosphate solutions without $(\text{NH}_4)_2\text{SO}_4$. The total current density 12.5 mA cm^{-2} .

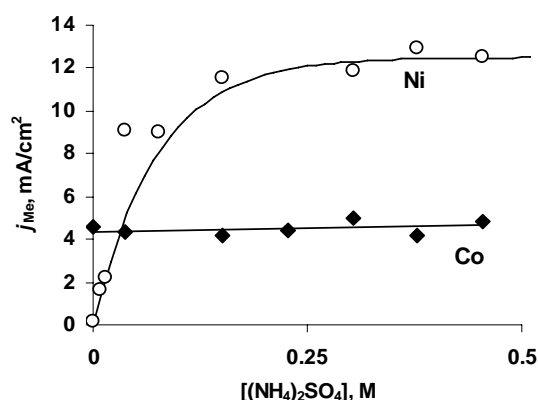
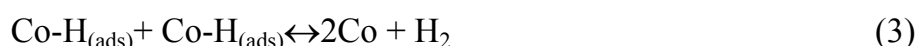


Fig. 8. The effect of initial $(\text{NH}_4)_2\text{SO}_4$ concentrations on partial current densities for Co and Ni at pH 8.0. Total current densities were: $j=45 \text{ mA/cm}^2$ for Co, and $j=30 \text{ mA/cm}^2$ for Ni.

Ammonium ions differently influence on the deposition rate of Ni and Co at given values of pH. Ni deposition rate sharply increases with increasing in concentration of ammonia up to 0.25 mol/l, and further increasing in ammonia concentration does not change the deposition rate sufficiently. Whereas, ammonia does not influencing the Co electrodepositing rate sufficiently. The characteristic results are shown in Fig. 8. The lower partial current densities for Co(II) are caused by the lower concentration of Co(II) in solution.

The different effect of ammonium sulfate on the deposition rate might be defined by the different origin of electrochemically active complex. There are three types of Me(II) complexes formed in the solutions that might participate as a charge transferring complexes, namely with pyrophosphate, with OH^- , and with ammonia, as well as hydrated ions Co^{2+} or Ni^{2+} . The rate of cobalt electrodeposition is sensitive to the pH irrespectively to the presence of complexes with ammonia and increases with increasing in pH up to pH 8. This fact confirms indirectly the role of hydroxo- complexes with Co(II), and especially Co monohydroxide CoOH^+ as a charge-transfer species. The concentration of these complexes linearly depends on pH that explains the obtained increasing rate of Co electrodeposition with pH. The side reaction of importance for iron-group metals electrodeposition is hydrogen evolution reaction under Volmer-Heyrovsky mechanism in alkaline media:



Actually, single iron group metal electrodeposition also can be described by the sequence of stages involved intermediate ion adsorption and interactions in adsorbed stage. The reaction pathway is assumed as follows:



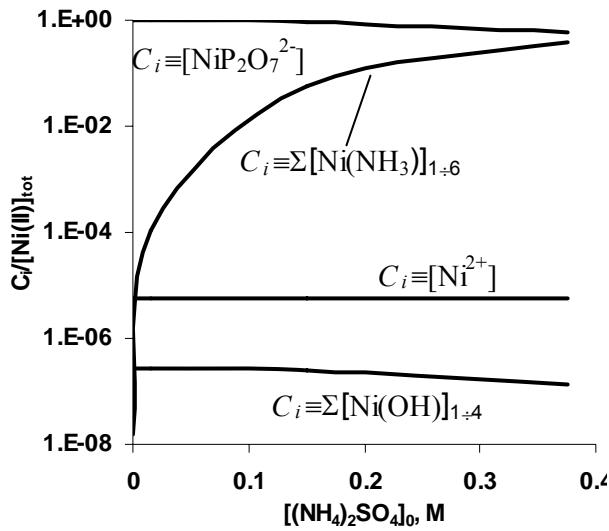


Fig. 9. Calculated molar fractions of some Ni(II) complexes (C_i) in total Ni(II) ($[\text{Ni(II)}]_{\text{tot}}$) as a function of total $(\text{NH}_4)_2\text{SO}_4$ concentration at pH 9. Solution composition: 0.36M $\text{Na}_4\text{P}_2\text{O}_7$ + 0.14M NiSO_4 + 0.3M ammonia.

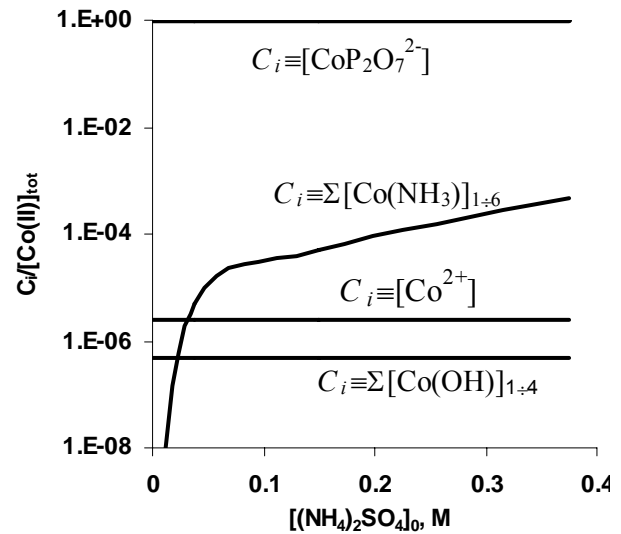


Fig. 10. Calculated molar fractions of Co(II) complexes (C_i) in total Co(II) ($[\text{Co(II)}]_{\text{tot}}$) plotted versus total $(\text{NH}_4)_2\text{SO}_4$ concentration at pH 9. Solution composition: 0.36M $\text{Na}_4\text{P}_2\text{O}_7$ + 0.025M CoSO_4 + 0.3M ammonia.

Increasing of pH in alkaline range facilitates hydrogen evolution reaction, also Co deposition rate increases due to increasing in concentration of CoOH^+ in the solution. However, because the competitive adsorption takes place, the Volmer's reaction occurs easier than reactions (4) or (5), therefore Co deposition rates drops down at higher pH.

Because of nickel does not electrodeposits without ammonia from pyrophosphate solutions at significant rates, no one of pyrophosphate or hydroxo – complexes with Ni(II) can be considering as a charge-transferring complex. Only after ammonium sulfate has been added, the Ni deposition rate increases sufficiently, and the deposition rate remains almost constant, if total concentration of ammonia > 0.2-0.3 M. Moreover, this result well-correlates with changes in total concentration of ammonia complexes with Ni(II): the fraction of complexes with NH_3 does not increases sufficiently if concentration of, ammonia exceeds 0.1-0.3 M – see Fig. 9.

3.2. Electrodeposition of Co-W

3.2.1. The selection of solution for Co-W electrodeposition

This study is intended to establish more details of relationship between electrodeposition parameters and CoW alloys composition and structure. As well the attempts to select and to improve existing procedures and plating bath formulations to deposit nanocrystalline coatings of CoW taking into account their possible application in MEMS had been made.

The citrate-boric bath for CoW alloy electrodeposition of main formulation $\text{Na}_2\text{WO}_4 \cdot 2\text{H}_2\text{O}$ - 0.05 M; $\text{CoSO}_4 \cdot 7\text{H}_2\text{O}$ - 0.2 M; $\text{C}_6\text{H}_8\text{O}_7$ - 0.04 M; $\text{Na}_3\text{C}_6\text{H}_5\text{O}_7$ - 0.25 M H_3BO_3 - 0.65 M, at pH 6.7 and 8.0, temperature 60 °C is convenient electrolyte: stable

composition of solution even at elevated temperatures, quite high electrodeposition rate is obtaining without stirring of solution.

The presence of non-metallic elements such as oxygen and carbon in tungsten alloys was reported in some publication. The presence of citric acid might cause the inclusion of carbon into alloys. The presence of oxygen on the top of alloy is explained by favourable oxide state of iron group metals and tungsten in air. We performed some experiment to prove this point of view. The electrodeposited Co-W alloys were kept in open air for 14 days, then analysis of top side. The analysis of rear side, adhered to substrate side, was followed by the exfoliation of deposit immediately prior the analysis. As is shown in Fig. 11, the peak related to oxygen and carbon does not appear on the rear side of alloy, because substrate and bulk deposit block it from exposure in air.

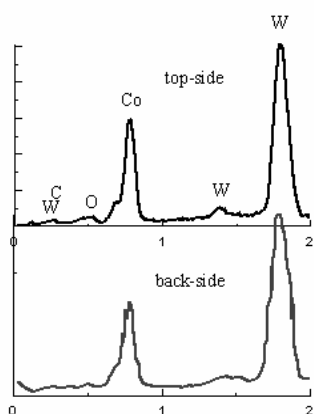


Fig. 11. EDX spectra of Co-W of top and rear side of deposit. The content of W on top and rear side is 18.25 and 16.4 at. %, respectively. Alloy has been deposited from the bath at pH 6.7 and $i=3 \text{ mA}\cdot\text{cm}^{-2}$.

3.2.2. Efefct of deposition conditions to Co-W composition and micro structure (direct current mode - DC)

The dependence of tungsten composition of CoW alloys deposition on the cathodic current density is shown in Fig. 12. Content of W increases sharply at pH 6.7 depending on the cathodic current density applied (fig. 12) reaching the maximum values of W in metallic phase of 30 at.%. That values correspond of minimum tungsten content at pH 8, where the tungsten increase slowly reaching 36 at.%.

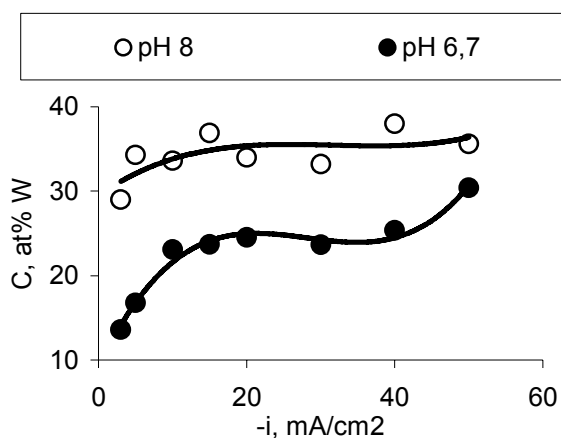


Fig. 12. Dependence of tungsten composition of electrodeposited CoW alloys on cathodic current density at different pH.

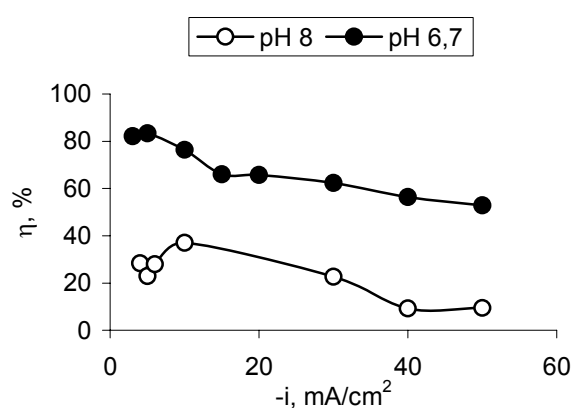


Fig. 13. Dependence of current efficiency on cathodic current density at different pH.

The decrease in the current efficiency at cathodic current density more than 10 A/cm² is caused by the evolution of hydrogen from the bulk of the electrolyte, which results in the decrease of current efficiency and hence the thickness.

Dependently on the electrodeposition conditions obtained alloys have different surface morphology. At DC mode and pH 6.7 and relatively low current densities obtained matic coatings with big crystallines. When cathodic current density increases and composition of alloys reach the >23% then the surface structure change and become more fine, and surface of coating become semi-glossy. At pH 8.0 W content in alloy reach ~30% and at surface glisten and have fine cristaline structure.

3.2.2. Co-W alloys electrodeposition at pulse current mode (PC)

In this investigation the amplitude of current density was the same $i_p = 30 \text{ mA/cm}^2$, but the average current density (i_{avg}) and pulse and pause duration were selected in that way that duty circle would be $T = 16,7\%$ and $33,3\%$. The dependences of W content in Co-W alloys on impulse duration are shown in fig. 14 and 15. At the average current density 5 mA/cm² W content in alloy depends on the pulse current conditions, but for average current density 10 mA/cm² the composition of alloy practically does not depend on the pulse current conditions.

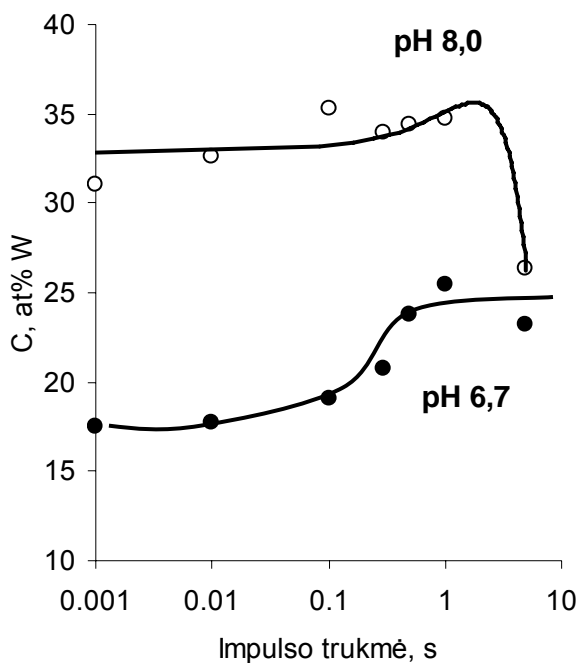


Fig. 14. Dependence of tungsten content in CoW alloys on the pulse duration at the different pulse duration and pH; $i_{avg} = 5 \text{ mA/cm}^2$ and $T = 16,7\%$.

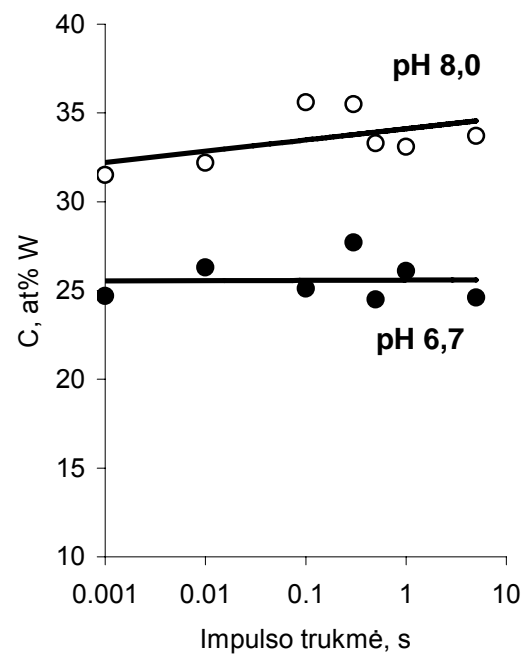


Fig 15. Dependence of tungsten content in CoW alloys on pulse duration at PC deposition at different pulse duration and pH $i_{avg} = 10 \text{ mA/cm}^2$ and $T = 33,37\%$.

3.2.3. Structure of Co-W alloys

The structure of obtained Co-W alloys was studied based on the obtained XRD patterns, and characteristic set of ones is shown in Fig. 16. XRD patterns indicate that CoW alloys with a crystalline structure were only deposited in solutions with pH 6.7 under low direct

current (DC) densities ($< 1 \text{ A dm}^{-2}$) or at the short pulse duration ($< 0.5 \text{ s}$) in the case of pulse current (PC) deposition. At higher current densities, longer pulse duration and in all the cases at pH 8.0 Co-W alloys with amorphous structure were formed. Coatings deposited under low DC densities ($< 1 \text{ A dm}^{-2}$) presented mixture of two crystalline phases: W solid solution in hcp Co and a small quantity of Co_3W also having hcp structure.

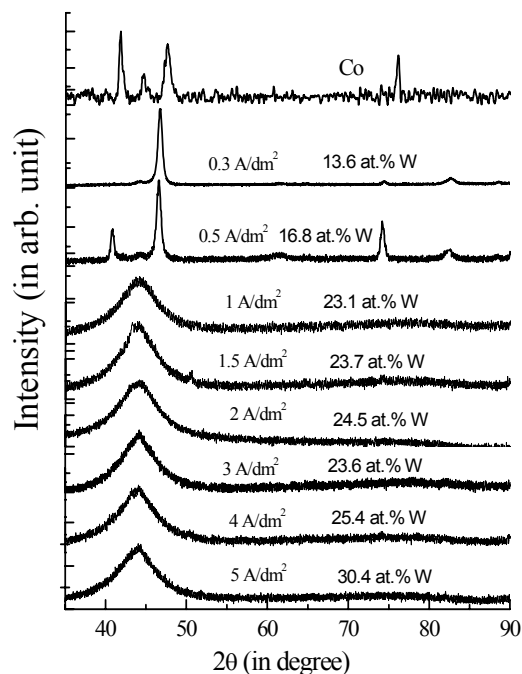


Fig. 16. XRD patterns obtained for Co-W alloys electrodeposited in DC mode at pH 6.7. Content of W and current density applied are indicated over corresponding curve.

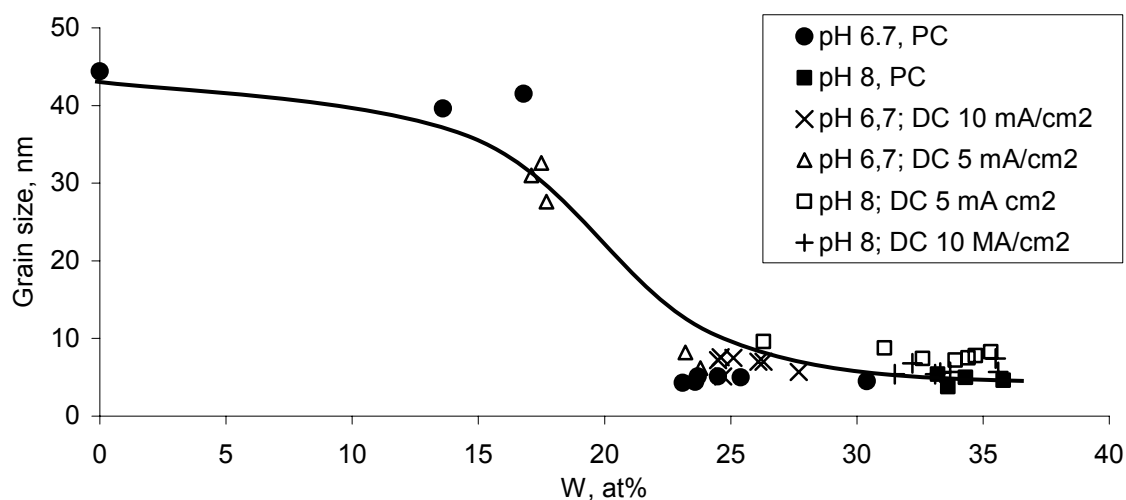


Fig. 17. The grain size of Co-W alloys as a function of W content in alloy at different electrodeposition conditions. Markings: „DC“ means direct current mode; „PC“ means pulse current mode, and numbers means average current density in PC mode.

The XRD peak broadening are related to grain size. Calculated values of grain size are summarized in fig. 17. As it is seen, the values of grain size depends on the W content in alloys regardless the electrodeposition conditions. When W content in alloy increases the grain size decreases from 45 nm (crystalline structure) to 4-6 nm (amorphous structure).

This decreasing is sharp and occurs in the narrow range of W content in alloy, namely at ~20-23 at.%, i.e. when Co_3W structure dominates.

3.3. Electrodeposition of CoMo and CoMoP alloys from the weakly acidic solutions

3.3.1. The study of Co-Mo alloys electrodeposition

Electrodeposition was carried out from the electrolytes of the following composition:

Solution 1: CoSO_4 (0.3 M) + $\text{Na}_3\text{Citr.}$ (0.2 M) + Na_2MoO_4 (0,005 M);

Solution 2: CoSO_4 (0.3 M) + $\text{Na}_3\text{Citr.}$ (0.2 M) + Na_2MoO_4 (0,012 M);

Solution 3: CoSO_4 (0.3 M) + $\text{Na}_3\text{Citr.}$ (0.2 M) + Na_2MoO_4 (0,012 M)+ NaH_2PO_2 (0,1M);

Solution 4: CoSO_4 (0.3 M) + $\text{Na}_3\text{Citr.}$ (0.2 M).

Current Efficiency and Deposition Rate. Figures 18 and 19 show the dependences of current efficiency and the deposition rate on the current density of Co-Mo alloys obtained from Solution 1 and 2. For comparison, the Fig. 20 and 21 show the dependence of the current efficiency and the deposition rate of pure Co coatings from electrolyte: CoSO_4 (0.3 M) + $\text{Na}_3\text{Citr.}$ (0.2 M) at the same current densities. One can be seen that the deposition rates for cobalt–molybdenum coatings are sufficiently lower; this is chiefly due to lower hydrogen overvoltage on Mo-containing electrodes. It is also obvious that the investigating solution have a high throwing power, because in a wide range of applied current densities the current efficiency falling down with the increase in current density at pH 4 and 5 (Fig. 18). At pH 5 (Fig. 19) this dependence give the practically identical rate of deposition that is favorable for the electrodeposition in recesses where local current density can be different at this is usually effect the uniformity of deposit grow.

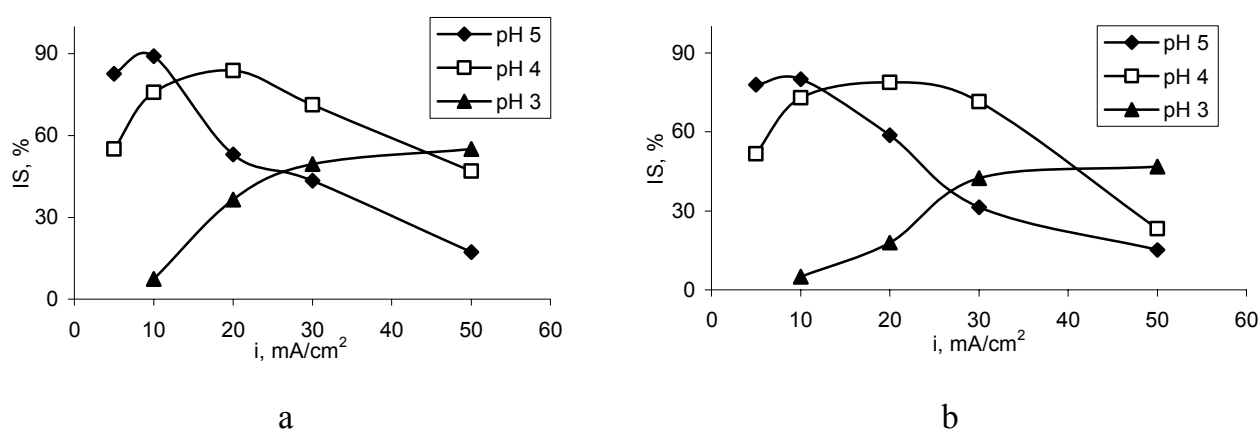


Fig.18. Influence of current density on current efficiency at various pH for Solution 1 (a) and Solution 2 (b), 1 – pH 3, 2 – pH 4, 3 – pH 5.

The change of electrodeposition potential by ~0.1-0.15V is evident at the higher current densities and at the beginning of electrodeposition. The rise of electrodeposition potential is caused probably by the enrichment of Mo in the depositing alloy after Cu substrate had been covered by first layers of Co-Mo. Further, the electrodeposition

potential becomes stable enough, and compositionally uniform alloys can be obtained through entire film thickness of Co-Mo.

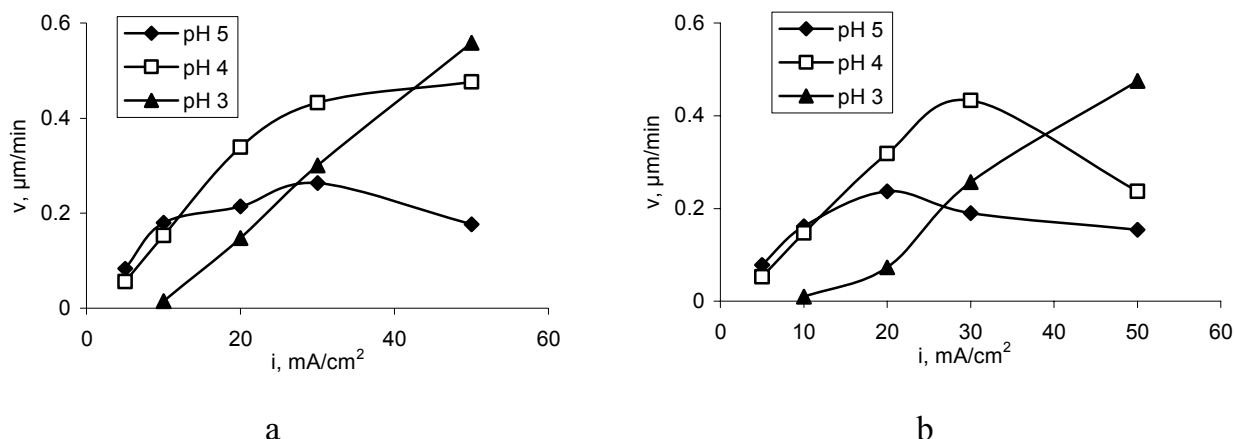


Fig.19. Influence of current density on deposition rate at various pH for Solution 1 (a) and Solution 2 (b), 1 – pH 3, 2 – pH 4, 3 – pH 5.

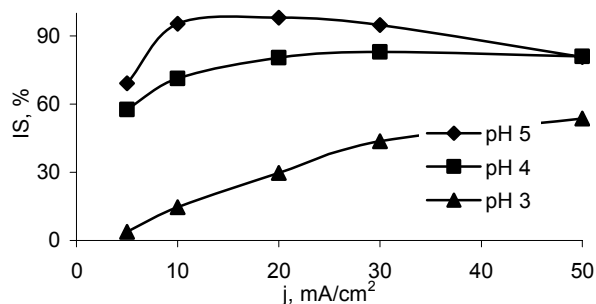


Fig. 20. Influence of current density on current efficiency at various pH for pure Co electrodeposition from Solution 4, 1 – pH 3, 2 – pH 4, 3 – pH 5.

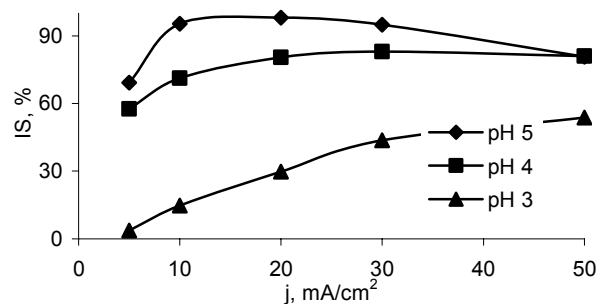


Fig. 21. Influence of current density on deposition rate at various pH for Solution 4, 1 – pH 3, 2 – pH 4, 3 – pH 5.

Morphology, Composition, and Structure of the Coatings. The electrodeposition conditions have influence on the morphology of the obtained coatings (Fig. 23). An increase in pH from 3 to 5 causes the increase in Mo content from 0.4 to 4.9 at.% (Solution 1). The same trend was obtained in Solution 2 where concentration of sodium molybdate is higher, that results a higher amount of Mo in the alloys. At relatively high (~ 5) pH and low amount of Mo in alloy, the deposits obtained at low current densities have needle-shaped surface (Solution 1). The surface becomes more flat when current density increases even at the similar amount of Mo in alloys (pH 4, Solution 1). The increase of Na_2MoO_4 concentration up to 0.012 M results in a flat surface even at low current densities and low amount of Mo in alloy (Solution 2). Noticeably, the obtained “needle” - shaped structure of Co-Mo alloys also is typical for pure Co electrodeposited from citrate baths (see Fig. 24).

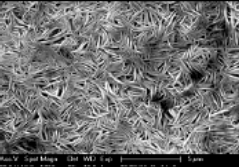
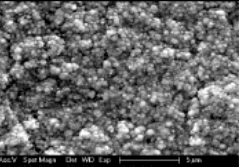
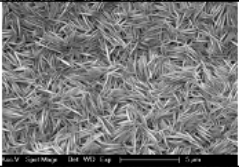
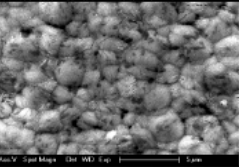
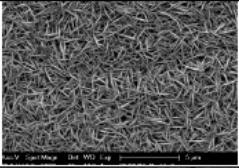
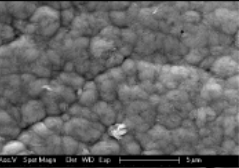
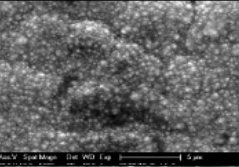
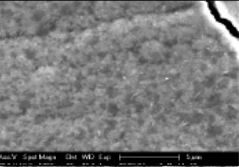
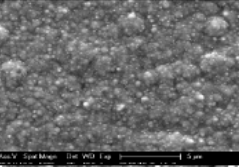
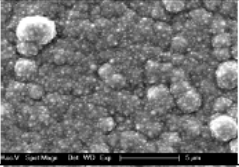
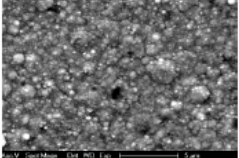
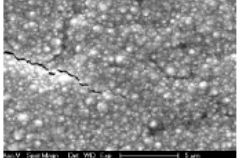
pH	i , mA/cm ²	Solution 1		Solution 2	
		Content of Mo in at. %			
5	2,5		4,9	11,4	
5	5		3,6	8,1	
4	2,5		1,6	3,9	
4	5		1,8	5,3	
3	12,5		0,7	0,8	
3	25		0,4	1,0	

Fig. 23. Surface morphology and content of Co-Mo alloys electrodeposited from the solution 1 and 2 at various pH.



Fig. 24. SEM image of pure Co electrodeposited from the citrate baths.

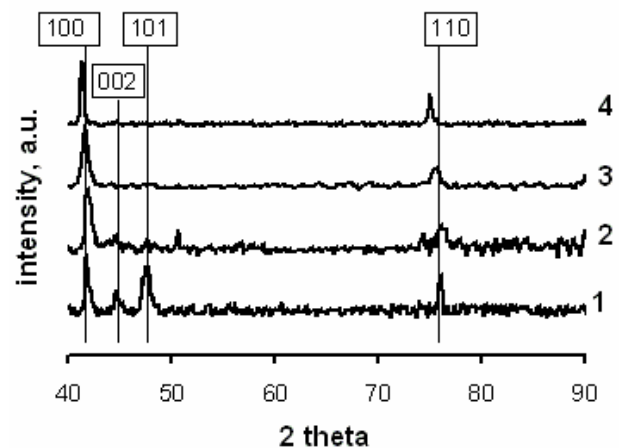


Fig. 25. XRD patterns for the electrodeposited from citrate baths pure Co (at 5 mA cm⁻²) and Co-Mo alloys. Lines mark positions of peaks attributed to the hexagonal Co in accordance with JCPDC data base. 1 – electrodeposited Co, 2 – Co-1.8 at.% Mo, 3 – Co-4.9 at.% Mo, 4 – Co-9.8 at.% Mo.

Co electrodeposited from citrate solutions has a hexagonal structure (see Fig. 25). The positions of XRD peaks of Co-Mo alloys may be attributed to the structure of hexagonal Co of dominating planes $\{100\}$ and $\{110\}$ as well. At higher concentration of Mo in the alloy (9.8 at. %) the XRD peaks shift to lower angles that is caused by the increase of interplanar distance of formed lattice from 2.16 Å (pure Co) to 2.18 Å (Co-9.8 at.% Mo) for texture $\{100\}$, and from 1.25 Å (pure Co) to 1.26 Å (Co-9.8 at.% Mo) for texture $\{110\}$.

As it is shown in Fig. 25 the broadening of peaks for the electrodeposited Co and electrodeposited Co-Mo alloys is similar; therefore the values of grain size for mentioned metals may be close to the values obtained for pure Co, i.e. ~ 40 nm.

3.3.2. Co-Mo-P alloys study concerning template-assisted electrodeposition

The hydrogen overvoltage on Mo and Mo-containing alloys is lower than that for W and W-containing alloys, therefore the current efficiency and deposition rate for Mo-containing alloys is lower than that for corresponding W-containing alloys. The accelerating rate of electrodeposition is important when template-assisted electrodeposition is concerned especially in the porous membranes or wafers with high aspect ratio. In this study we selected sodium hypophosphite as accelerator, because introduction of some amount of phosphorous into alloys does not have adversary effect on the surface morphology and corrosion properties of alloys even if the introduction of phosphorous occurs in cost of molybdenum.

The effect of NaH_2PO_2 on the polarization at various pH is shown in Fig. 26. It can be seen, the accelerating effect in the presence of NaH_2PO_2 is more evident at lower values of pH although at pH 8 the acceleration takes place. It is caused probably by the easier reduction of hypophosphite ion at lower pH and incorporation of P into alloy that change the kinetics of Co and Mo codeposition.

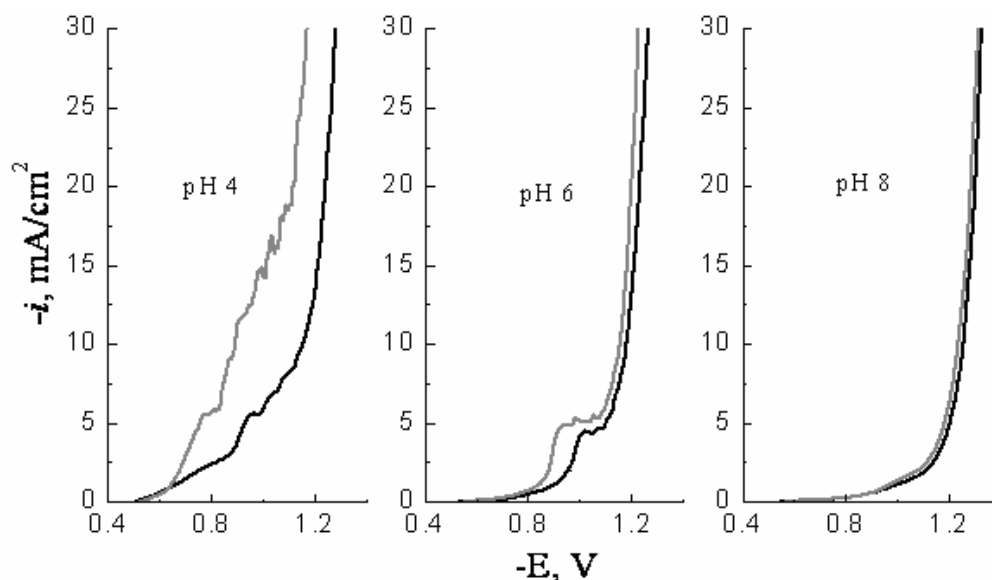


Fig. 26. Polarization curves registered on Co electrode from Solution 2 without NaH_2PO_2 (black curves) and from Solution 3 with NaH_2PO_2 (grey curves) at various pH. Potential scan rate 5 mV s^{-1} .

The plateau is obtained on the polarization curves determined in acidic solutions at current density 4-5 mA/cm². The origin of plateau obtained on the polarization curves needs further investigations. Based on the simple estimations of limiting diffusion current taking into account that concentration of Co(II) is 0.3M, the values of the diffusion limiting current have reach values 45-50 mA/cm². Preliminary study by means of EIS also does not show the slow diffusion stage because Warburg impedance does not appear in spectra. Most probably, the plateau is caused by the adsorbed intermediate compounds participating in the charge transfer reaction.

In all cases the currents are higher for electrodeposition in the present of NaH₂PO₂ that is more favorable for electrodeposition in wafers that require long time, but quality of deposits obtained at pH 4 is worse than obtained at higher pH. The summation of the influence of the electrodeposition parameters and presence of hypophosphite on the quality of the obtained coatings at pH 6 is following:

- the presence of phosphorous in the alloys obtained at direct current do not influence on the surface morphology, but the deposition rate of ternary alloy is sufficiently higher than that for binary with molybdenum;
- ternary alloys containing P and electrodeposited in pulse current mode have less stress and cracks especially electrodeposited at low average current density.

3.3.3. Electrodeposition into wafers:

The thickness and content uniformity of electrodeposited metals and alloys applied in interconnect metallization of semiconductor wafers is of importance. Variations must be typically kept below ~ 3%, with only a few millimeters edge exclusion. A number of process parameters, including the resistive copper seed and the wafer and anode configurations that are controlled by practical design considerations, adversely affect the current distribution. An important issue during MEMS processing is the ability to plate and fill high aspect ratio structures evenly, and void free filled trench. Conformal plating is an even growth from all surfaces resulting in a deposit of equal thickness at all points.

Table 3. The deposition parameters and composition of Co-Mo-P alloys obtained from Solution 3.

Sample	pH	$C_{NaH_2PO_2}$ M	i_{avg} , mA/cm ²	i_p , mA/cm ²	t_{ON} , s	t_{OFF} , s	v , μ m/min	Composition at. %		
								Co	Mo	P
a	6	0	4	-	continuous	0	0.170	73.9	26.1	-
b		0.1	4	-	continuous	0	0.287	81.9	12.6	5.5
c			4	12	5	10	0.226	86.1	8.5	5.4
d			1.3	4	5	10	0.141	87.7	7.6	4.7

The wafers used in this study have photoresist layer over copper and patterned by the mask. This mask had opening squares whose size is 100 x 100 μ m and 20 μ m deep. Finally the Co-Mo-P alloys were plated under such optimal conditions: pH 6, averaged current density $i_{avg} = 4$ mA/cm², pulse current density, $i_p = 12$ mA/cm² and t_{ON}/t_{OFF} is

5s/10s. These conditions correspond to the electrodeposition on bulk samples as shown in table 3, sample c. As follows from the data presented in Table 3, when the amount of phosphorous in the alloys increases, the ratio of Mo:Co is reduced sufficiently, i.e. content of Mo in the alloy decreases sufficiently.

The general and detailed SEM images of filling recesses after photoresist had been dissolved are shown in Fig. 27. As it is seen, the filling of the recesses is reasonable; the height of obtained posts is the uniform (Fig. 27 a and b); the surface is flat and consists on the fine crystallites (Fig. 27 e and f). The evenness of alloy composition distribution was estimated by measuring the composition in different places. It was found that for the resulting alloy with composition (in at. %) Co-9.3Mo-3.5P, the variation of analysis data does not exceeds $\pm 5\%$ of determined value.

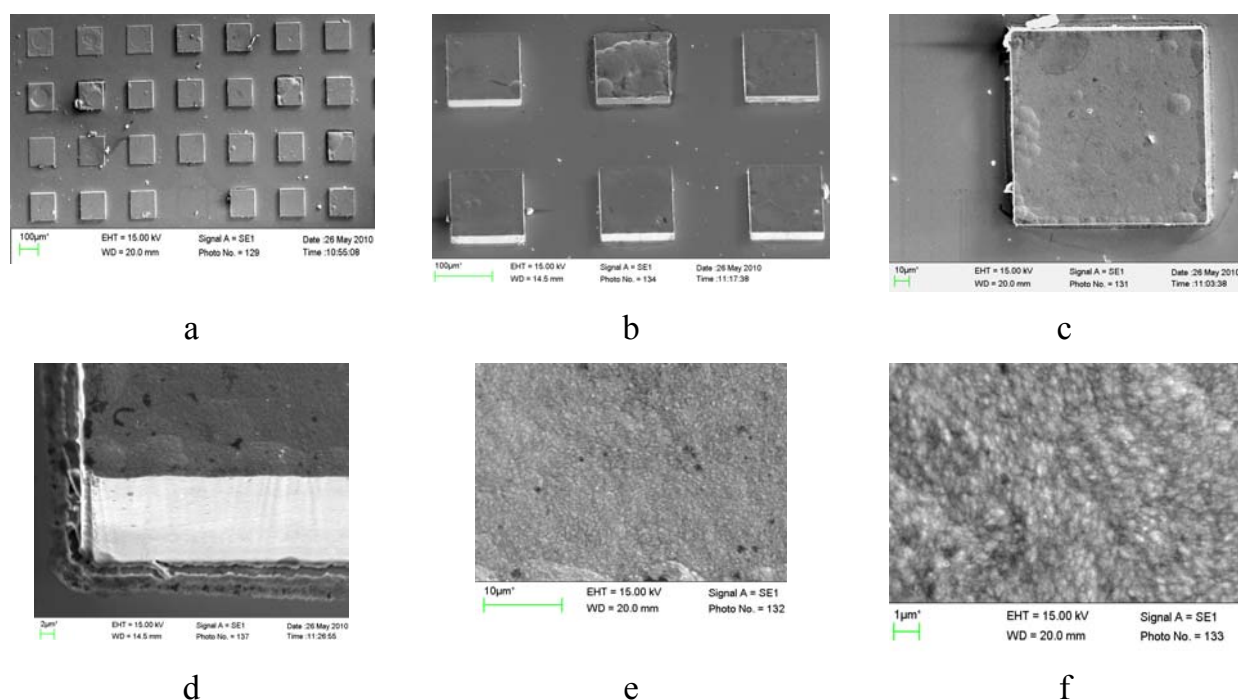


Fig. 27. SEM images of the big fragment of wafer (a), and detailed images of wafer with recesses filled by Co-Mo-P alloy (b, c and d), and the morphology of tops (e and f). Content of alloy Co-9.3 at.% Mo-3.5 at.% P.

3.3. Hydrogen evolution and corrosion of W and Mo alloys with Co and Ni

The electrodeposition of W and Mo alloys were performed on the mechanically polished copper. Co-W alloys were electrodeposited at 70°C from citrate-borate baths containing 0.2M CoSO₄·+0.2M Na₂WO₄·+ 0.04M C₆H₈O₇+0.25M Na₃C₆H₅O₇ +0.65M H₃BO₃.

The contents of investigated Co-W alloys and their electrodepositing conditions are presented in Table 4. The contents of obtained Co-W alloys was selected in such way that content of W would vary in the wide range either at the similar deposition condition (samples No. 2 and 5) or remains approximately the same at the different electrodeposition conditions (samples No. 3 and 4).

The electrochemical hydrogen evolution depends on the both chemical composition and surface state of electrode. The highest values of hydrogen overvoltage were obtained on

cast Co and W, and the lowest hydrogen overvoltage possesses pure Co electrodeposited from citrate-borate bath. The obtained potentials of hydrogen evolution for Co-W are in the relatively narrow range of potentials. The data obtained for Sample No. 7, electrodeposited at low frequency pulse deposition mode, are outstanding. However, this result is well-reproducible, and probably is related with the structural peculiarities of obtained alloy, and need a further study.

Table 4. Electrodeposition conditions and contents of Co-W alloys. “DC” and “PC” means direct current and pulse current electrodeposition modes, respectively.

Sample No.	Metal	Content of W, at%	Electrodeposition mode	Pulse duration in PC mode, s	Current density, mA/cm ²	pH of solution
1	Co (electrodeposited)	0	DC		10	6.7
2	CoW	16.40	DC		3	6.7
3	CoW	17.70	PC	0.01	5	6.7
4	CoW	19.14	PC	0.1	5	6.7
5	CoW	21.20	DC		10	6.7
6	CoW	24.50	PC	0.5	10	6.7
7	CoW	24.56	PC	5	10	6.7
8	CoW	31.09	PC	0.001	5	8.0
9	CoW	33.33	PC	0.5	10	8.0
10	CoW	35.60	PC	0.1	10	8.0
11	W (cast wire)	100				
12	Co (cast, wire)	0				

The values of the exchange current densities for hydrogen evolution were determined by the extrapolation of Tafel plot to the value of Nernst potential for the system H_2/H^+ . The value of the Nernst potential for hydrogen evolution in the investigated media is -0.298 V. The values of Tafel coefficient “b” for Co-W alloys are in the range 0.09-0.13 V. The values of exchange current density as a function of W content in Co-W alloys are presented in Fig. 28. This dependence has a minimum at 24-30 at.% of W. This range of tungsten contents in Co-W alloys is transitive from the polycrystalline structure to nanocrystalline.

Ni-Mo alloys were electrodeposited at the room temperature and pH 8.5 from pyrophosphate baths containing 0.14M $NiSO_4$ + 0.004÷0.04M Na_2MoO_4 + 0.35 M $Na_4P_2O_7$ + 0.4M NH_4Cl . The same methodology for investigation was applied to Ni-Mo alloys as well. The contents of investigated Ni-Mo alloys are presented in Table 5. Both pure nickel (cast and electrodeposited) and pure molybdenum possess higher hydrogen overvoltage than Ni-Mo alloys, i.e. these alloys show catalytic evolution of hydrogen, in contrary to Co-W alloys.

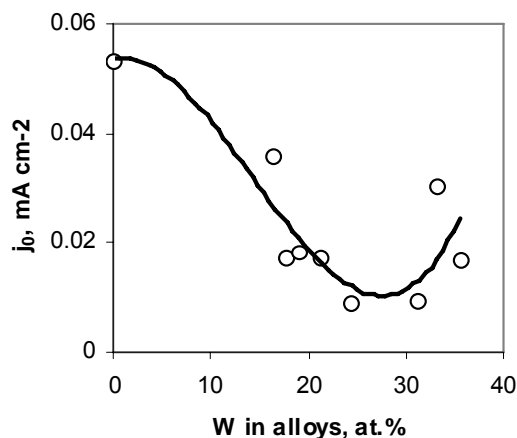


Fig. 28. Exchange current density for hydrogen evolution as a function of W content in Co-W alloys.

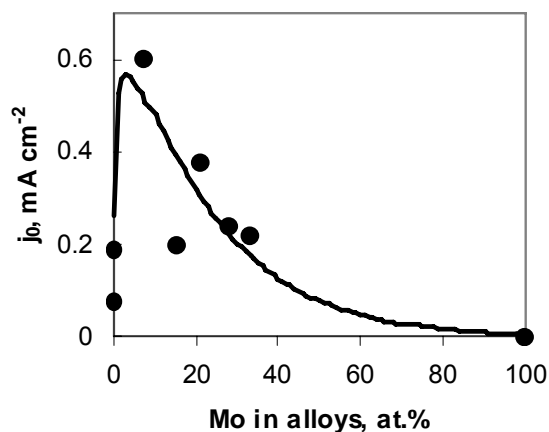


Fig. 29. Exchange current density for hydrogen evolution as a function of Mo content in Ni-Mo alloys.

Table 5. Contents of Ni-Mo alloys used for the study.

Sample No.	Metal	Mo at%
1	Ni (electrodeposited)	0
2	NiMo	7.5
3	NiMo	15
4	NiMo	21
5	NiMo	28
6	NiMo	33
7	Ni (cast wire)	0
8	Mo (cast wire)	100

The exchange current densities for hydrogen evolution reaction on Ni-Mo alloys are sufficiently higher than that on Co-W (see Fig. 29) regardless the lit bit higher values of Tafel coefficient “b” that values are in the range 0.11-0.15V. This dependence on the Mo content in alloys has a maximum at 5-8 at.% of Mo in alloys, i.e. the catalytic effect on the hydrogen evolution is most pronounced. Ni-Mo alloys at such contents of Mo have polycrystalline structure, whereas nanocrystalline Ni-Mo alloys show lower exchange current density for hydrogen evolution.

The corrosion rate of obtained alloys was estimated based on the voltammograms obtained in 0.5M H₂SO₄ solution. As the shape of voltammograms is asymmetric, therefore it is impossible to estimate corrosion rate of corresponding alloys by extrapolating lines in Tafel region. In this study the each curve was transformed into Allen-Hickling coordinates that enable to estimate a corrosion rate using narrow range of potentials.

Interestingly, both for Co-W alloys and Ni-Mo alloys corrosion potentials are similar irrespectively on the content of alloys. Moreover, the corrosion potentials for cast metals

are more positive than that for electrodeposited. The values of corrosion currents are summarized in Table 6.

Table 6. Electrodeposition conditions and contents of Co-W alloys. “DC” and “PC” means direct current and pulse current electrodeposition modes, respectively.

Sample No.	Metal	Content of W, at%	Corrosion current, mA cm ⁻²	Sample No.	Metal	Content of W, at%	Corrosion current, mA cm ⁻²
1	Co (electrodepos.)	0	0.232	1	Ni (electrodepos.)	0	0.068
2	CoW	16.40	0.008	2	NiMo	7.5	0.058
3	CoW	17.70	0.015	3	NiMo	15	0.050
4	CoW	19.14	0.014	4	NiMo	21	0.058
5	CoW	21.20	0.019	5	NiMo	28	0.123
6	CoW	24.50	0.062	6	NiMo	33	0.037
7	CoW	24.56	0.151	7	Ni (cast wire)	0	0.043
8	CoW	31.09	0.040	8	Mo (cast wire)	100	0.006
9	CoW	33.33	0.037				
10	CoW	35.60	0.046				
11	W (cast wire)	100	0.003				
12	Co (cast, wire)	0	0.057				

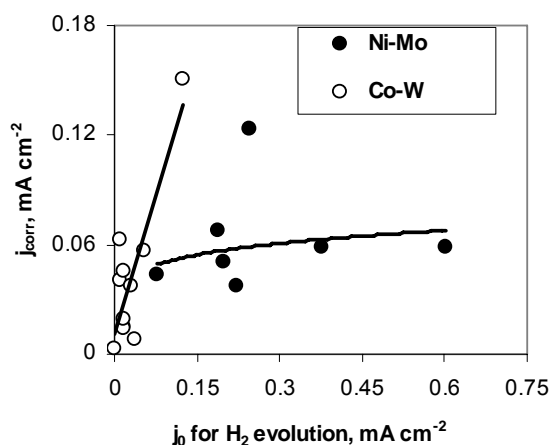


Fig. 30. Corrosion currents densities vs. H₂ exchange current densities for Co-W and Ni-Mo alloys.

As follows from the data presented in Table 6, the corrosion current densities for both Co-W and Ni-Mo alloys are of the same level. The correlation between exchange current density for hydrogen evolution and corrosion current is presented in Fig. 30. As follows from the obtained data, for Co-W alloys the clear correlation between exchange current for H₂ evolution is obtained, whereas for Ni-Mo alloys such correlation is rather weak. The weak correlation for Ni-Mo alloys is caused by the higher values of Tafel coefficients that yield to faster decrease in current in the vicinity of corrosion potential.

4. CONCLUSIONS

1. The shape of voltammograms obtained for the electroreduction of Co(II) and Ni(II) look like in the case of mixed kinetics (slow charge transfer + diffusion), and plateau presences on the curves. However the study by means of electrochemical impedance spectroscopy yields the absence of diffusion limitations. The obtained EI spectra are fitted well to the equivalent circuits simulating the slow charge transfer in the presence of the adsorption of intermediate compound.
2. Ni electrodeposition rate from pyrophosphate baths without ammonia is extremely small. Adding of $(\text{NH}_4)_2\text{SO}_4$ and further forming of ammonia in the solution accelerates sufficiently the rate of Ni electrodeposition. The effect well correlates with increasing the molar fraction of various ammonia complexes with Ni(II). Whereas, the rate of Co electrodeposition is much higher, the presence of ammonia does not influence the deposition rate. However, the Co deposition rate is sensitive to pH. Based on the different pH and $(\text{NH}_4)_2\text{SO}_4$ influence on the deposition rate it is possible to assume that CoOH^+ and $\text{Ni}(\text{NH}_3)_{1-6}^{2+}$ can act as a charge-transfer particles in the pyrophosphate-ammonia solutions.
3. The dependences of Co-W content and structure on the electrodeposition conditions were determined. The grain size depends rather on W content than on the electrodeposition conditions. At lower content of W (<20 at.%), Co-W alloy is polycrystalline (grain size > 30 nm), and when $W > 22$ at.%, the grain size drops down to <6 nm in the narrow range of W contents. Regardless the content of W (if it is >13 at.%), the structure of Co-W is the same as the intermetallic compound Co_3W .
4. The deposition rates for Co-Mo coatings are sufficiently lower than that for pure cobalt. The alloys containing up to 10 at.% of Mo were electrodeposited. At relatively high (~5) pH and low amount of Mo in alloy, the coatings deposited at low current densities have needle- shaped surface. The surface becomes more flat when current density increases even at the similar amount of Mo in alloys (pH 4). The deposition rate increases sufficiently when ternary Co-Mo-P alloys are electrodeposited. The structure of obtained Co-Mo alloys is the same as for hexagonal Co.
5. For the electrodeposition in wafers the low frequency current pulse mode was chosen. The alloy having composition (in at. %) Co-9.3Mo-3.5P was electrodeposited. The filling of the recesses is reasonable, and the height of obtained posts is the same, and the surface is flat and consists on the fine crystallites.
6. Exchange current density for hydrogen evolution as a function of the content of Co-W alloys has a minimum corresponding to transitive from polycrystalline to nanocrystalline structure. For Ni-Mo alloys this exchange current density is higher than that for a pure component of alloys, i.e. the catalytic evolution of hydrogen is occurring in the case of Ni-Mo alloys. The values of corrosion current are similar for both Co-W and Ni-Mo alloys. For Co-W alloys the clear correlation between exchange current for H_2 evolution is obtained, whereas for Ni-Mo alloys such correlation is rather weak.

The list of Original publications by the Author

Articles in journals

1. H.Cesiulis, **A.Budreika**, Electroreduction of Ni(II) and Co(II) from Pyrophosphate Solutions// *Materials science - Medziagotyra*, 2010, vol. 16, No. 1, 52-56.
2. H.Cesiulis, **A.Budreika**, Hydrogen evolution and corrosion of W and Mo alloys with Co and Ni // *Physicochemical Mechanics of Materials* (ISSN 1392-1320), 2010, No. 8, 808-814.
3. H. Cesiulis, N. Tsyntsaru, **A. Budreika**, N. Skridaila, Electrodeposition of Co-Mo alloys from the weakly acidic solutions// *Surface Engineering and Applied electrochemistry* (ISSN 0013-5739), 2010, No. 5, 17-26.

Published contributions to academic conferences:

4. H. Cesiulis, **A. Budreika**, I. Prosyčėvas, N. Tsyntsaru, S. Belevsky. Co-W lydinių elektronusodinimas iš citratinių elektrolitų // *Neorganinių junginių chemija ir technologija. Konferencijos pranešimų medžiaga*. Kaunas, 2009, p. 13-16.

CIRRICULUM VITAE

Andrius Budreika

1996 – 2000 Bachelor studies at Vilnius University – Bachelor Degree in Chemistry.

2000 – 2003 Master Studies at Vilnius University – Master Degree in Chemistry.

2005 – 2009 Post – graduate studies at the Department of Physical Chemistry of Vilnius University.

Ni, Co bei jų lydinių su volframu ir molibdenu elektronusodinimo tyrimas

SANTRAUKA

Buvo tiriama Co(II) ir Ni(II) įvairių kompleksų elektoredukcija chloridiniuose, sulfatiniuose, citratiniuose, pirofosfatiniuose bei pirofosfatiniuose-amoniakiniuose tirpaluose, Ni ir Co lydinių su W ir Mo elektronusodinimas, gautų dangų sudėtis ir paviršiaus morfologija, struktūra bei korozinės savybės. W ir Mo lydiniai buvo nusodinami iš citratinių - boratinių - pirofosfatinių – amoniakinių elektrolitų, o koroziniai tyrimai atlikti sulfatiniuose tirpaluose.

Tiriant Co(II) ir Ni(II) elektoredukciją nustatyta, kad voltamperinių kreivių forma primena būdingas mišriai kinetikai voltamperines kreives, jose yra ryškus persilenkimas. Tačiau tyrimai EIS metodu parodė, kad šio persilenkimo negalima sieti su difuziniais apribojimais. Padaryta prielaida apie elektrochemiškai aktyvaus Co arba Ni komplekso lėtą adsorbiciją ant elektrodo. Nustatyta, kad Ni elektronusodinimo greitis iš pirofosfatinių tirpalų be amonio jonų yra labai mažas. Pridėjus $(\text{NH}_4)_2\text{SO}_4$ ir taip formuojant amoniakinius nikelio kompleksus tirpale, labai pagreitėja Ni elektronusodinimas. Šis efektas labai gerai koreliuoja su didėjančia apskaičiuotų įvairių Ni (II) kompleksų su amonio jonais frakcija. Tačiau amonio jonų buvimas praktiškai neturi įtakos Co elektronusodinimo greičiui. Iš gautų duomenų daroma išvada, kad elektrochemiškai aktyvus Ni ir Co kompleksai yra skirtingi, t.y. CoOH^+ ir $\text{Ni}(\text{NH}_3)_{1-6}^{2+}$ yra krūvį pernešančios dalelės pirofosfatiniuose – amoniakiniuose tirpaluose.

Nustatytos Co-W lydinio sudėties ir struktūros priklausomybės nuo elektronusodinimo sąlygų. Gautų Co-W lydinių kristalitų dydis labiau priklauso nuo volframo kiekio lydinio nei nuo elektronusodinimo sąlygų: kai W kiekis mažesnis nei 20 at.%, tuomet Co-W lydinis laikytinas kristaliniu (kristalitų dydis >30 nm), o kai $W > 22$ at. %, tuomet Co-W lydiniai yra nanokristaliniai („pseudoamorfiniai“), kurių kristalitų dydis <6 nm, ir perėjimas iš vienos būsenos į kitą yra staigus, jis vyksta W kiekiui lydinyje keičiantis 20-22 at. % ribose.

Tiriant Co-Mo ir Co-Mo-P lydinius nusodintus iš silpnai rūgščių citratinių elektrolitų, buvo nustatyta, kad Co-Mo dangų elektronusodinimo greitis yra daug mažesnis nei gryno Co, o nusodinant Co-Mo-P, naudojant natrio hipofosfitą lydinio nusodinimo greitis žymiai padidėja. Esant $\text{pH} \sim 5$ buvo gauti lydiniai, turintys mažai Mo; esant mažiems srovės tankiams paviršiuje formuojasi adatinė struktūra, o esant didesniems – blizgančioms dangoms būdinga sferoidinė struktūra. Padidinus Na_2MoO_4 koncentraciją iki 0.012 M gaunamos lygios dangos. Lydinio nusodinimui mikrostruktūrizuotuose silikoniniuose šablonuose panaudotas žemo dažnio impulsinės srovės režimas. Gautas lydinys, kurio sudėtis Co-9.3Mo-3.5P (at. %), ertmių užpildymo aukštis vienodas, paviršius lygus ir vienalytis.

Vandenilio skyrimosi mainų srovės tankio priklausomybė nuo Co-W lydinio sudėties turi minimumą, kuris susijęs su perėjimu nuo polikristalinės į nanokristalinę struktūrą. Ni-Mo lydinio šios mainų srovės tankis yra didesnis nei gryno lydinio elementų atskirai ir pasižymi katalitiniu vandenilio skyrimosi. Co-W atveju stebima aiški korozijos srovės priklausomybė nuo vandenilio skyrimosi mainų srovės, tuo tarpu Ni-Mo atveju tokia koreliacija nepastebėta. Co-W ir Ni-Mo lydinių korozijos srovės yra panašios.